JCI insight

RESEARCH ARTICLE

Sonic hedgehog connects podocyte injury to mesangial activation and glomerulosclerosis

Dong Zhou,[1] Haiyan Fu,[2] Yang Han,[2] Lu Zhang,[3] Shijia Liu,[4] Lin Lin,[1] Donna B. Stolz,[5] and Youhua Liu[1,2]

[1]Department of Pathology, University of Pittsburgh School of Medicine, Pittsburgh, Pennsylvania, USA. [2]State Key Laboratory of Organ Failure Research, National Clinical Research Center of Kidney Disease, Nanfang Hospital, Southern Medical University, Guangzhou, China. [3]Department of Nephrology and [4]Department of Clinical Pharmacology, Affiliated Hospital of Nanjing University of Chinese Medicine, Nanjing, China. [5]Department of Cell Biology and Physiology, University of Pittsburgh School of Medicine, Pittsburgh, Pennsylvania, USA.

Glomerular disease is characterized by proteinuria and glomerulosclerosis, two pathologic features caused by podocyte injury and mesangial cell activation, respectively. However, whether these two events are linked remains elusive. Here, we report that sonic hedgehog (Shh) is the mediator that connects podocyte damage to mesangial activation and glomerulosclerosis. Shh was induced in glomerular podocytes in various models of proteinuric chronic kidney diseases (CKD). However, mesangial cells in the glomeruli, but not podocytes, responded to hedgehog ligand. In vitro, Shh was induced in podocytes after injury and selectively promoted mesangial cell activation and proliferation. In a miniorgan culture of isolated glomeruli, Shh promoted mesangial activation but did not affect the integrity of podocytes. Podocyte-specific ablation of Shh in vivo exhibited no effect on proteinuria after adriamycin injection but hampered mesangial activation and glomerulosclerosis. Consistently, pharmacologic blockade of Shh signaling decoupled proteinuria from glomerulosclerosis. In humans, Shh was upregulated in glomerular podocytes in patients with CKD and its circulating level was associated with glomerulosclerosis but not proteinuria. These studies demonstrate that Shh mechanistically links podocyte injury to mesangial activation in the pathogenesis of glomerular diseases. Our findings also illustrate a crucial role for podocyte-mesangial communication in connecting proteinuria to glomerulosclerosis.

Introduction

Glomerular disease accounts for the vast majority of chronic kidney diseases (CKD) that eventually progress to end-stage renal failure (1–3). Despite different etiologies, most glomerular diseases are manifested clinically by proteinuria and glomerulosclerosis, two pathologic features caused by podocyte injury and mesangial cell activation, respectively (4, 5). Common glomerular diseases, such as focal and segmental glomerulosclerosis (FSGS) and diabetic kidney disease (DKD), begin with podocyte damage leading to proteinuria but often end up with glomerulosclerosis, which is initiated by mesangial cell activation, matrix overproduction, and scar formation (6, 7). However, whether and how podocyte damage links to mesangial cell activation remains elusive.

The relationship between proteinuria and glomerulosclerosis in the clinical setting is complex and not always straightforward (8, 9). In most circumstances, heavy proteinuria is one of the most well-recognized independent risk factors for CKD progression and poor prognosis (10, 11). However, patients with proteinuria are not necessarily destined to develop renal deficiency, characterized by functional decline and tissue fibrosis. This perplexity makes it difficult and not acceptable to use proteinuria as a surrogate marker for monitoring an outcome of clinical trials (12, 13). In this context, delineation of the molecular mechanisms underlying the possible connection between proteinuria and glomerulosclerosis will not only provide insights into the pathomechanisms of CKD, but also will be instrumental in designing effective treatments.

One hypothesis explaining the potential coupling of proteinuria with glomerulosclerosis is that the injured podocytes may secrete pathogenic factors, which cause mesangial cell activation through mediating

Conflict of interest: The authors have declared that no conflict of interest exists.

Submitted: May 22, 2019
Accepted: October 8, 2019
Published: November 14, 2019.

Reference information: *JCI Insight*. 2019;4(22):e130515. https://doi.org/10.1172/jci.insight.130515.

podocyte-mesangial communication. While this speculation appears plausible and attractive, the identity of such a factor remains to be unraveled. In the present study, we investigated the possibility that sonic hedgehog (Shh) may act as a mediator that links podocyte injury to mesangial cell activation and glomerulosclerosis in proteinuric CKD.

Hedgehog signaling is an evolutionarily conserved, developmental signal cascade that regulates a diverse array of biological processes in embryonic development, tissue homeostasis, and injury repair (14, 15). Among the 3 hedgehog ligands, Shh is the most widely studied and best characterized. Shh is synthesized as a precursor and then undergoes autocatalytic processing and posttranslational modifications in the producing cells, which are important for its proper trafficking, secretion, and receptor interaction. We and others recently reported that Shh is induced in renal tubular epithelium in obstructive and ischemic nephropathy (16–20) but targets to interstitial fibroblasts, leading to their activation and matrix production (17). These observations prompted us to test whether Shh also plays a role in coupling podocyte injury to glomerulosclerosis through mediating podocyte-mesangial communication.

Here, we report that Shh is induced specifically in the glomerular podocytes in various animal models of proteinuric CKD and in patients. Genetic ablation or pharmacologic inhibition of Shh represses mesangial activation and alleviates glomerulosclerosis but exhibits no effects on proteinuria. Our studies illustrate that podocyte injury is intricately linked to mesangial activation and glomerulosclerosis via Shh ligand.

Results

Shh is induced in podocytes but selectively targets mesangial cells in vivo. We first investigated Shh expression in various models of proteinuric CKD by immunohistochemical staining. As shown in Figure 1A, little or no Shh expression was found in the glomeruli of normal adult mice. However, a marked induction of Shh protein was evident in the glomeruli of injured kidney in various models of CKD, including adriamycin (ADR) nephropathy, anti–glomerular basement membrane (anti-GBM) disease, and DKD (Figure 1, A and B). Based on cell morphology and localization in the glomeruli, it appears that the Shh^+ cells were podocytes (Figure 1A, arrows). To further clarify this, we performed double staining for Shh and nestin, a podocyte-specific marker (21). As shown in Supplemental Figure 1 (supplemental material available online with this article; https://doi.org/10.1172/jci.insight.130515DS1), Shh was colocalized with nestin in the glomerular podocytes of diseased kidney. We then sought to confirm the functional activity of Shh signaling in vivo. To this end, we examined renal expression of Gli proteins, the transcriptional regulators that are downstream mediators and, when analyzed, can act as a read-out of hedgehog signaling. As shown in Figure 1C, quantitative real-time PCR (qPCR) assay revealed that both Gli1 and Gli2 were significantly induced in the kidneys after ADR injury.

To identify the upstream signal responsible for Shh induction in podocytes, we examined the potential role of Wnt ligands using cultured podocytes in vitro, because earlier studies showed that this signal cascade is activated in podocytes after injury (22, 23). As shown in Figure 1, D and E, multiple Wnt ligands, either alone or in combination, induced Shh expression in cultured mouse podocytes. Notably, conditioned media collected after transfection with multiple Wnt expression vectors dramatically stimulated Shh expression in vitro (Figure 1, D and E).

To delineate which cell responds to Shh stimulation in the glomeruli in vivo, we used $Gli1^{lacZ}$ reporter mice, which harbor a β-Gal–knockin mutation. Under the control of the native Gli1 promoter, lacZ expression in these mice authentically recapitulates the expression of endogenous Gli1 mRNA (17). As shown in Figure 1, F and G, X-Gal staining illustrated $\beta\text{-Gal}^+$ cells localized in the mesangial area at 1 week after ADR injection or 2 weeks after angiotensin II infusion. To ascertain the identity of the $X\text{-Gal}^+$ cells, we further carried out double immunostaining for endothelial cell marker CD31 and podocyte marker podocalyxin. As shown in Supplemental Figure 2, there was no colocalization of X-Gal with either CD31 or podocalyxin, suggesting that Shh is likely to target nonpodocyte and nonendothelial glomerular cells in vivo.

Shh specifically promotes mesangial cell activation and proliferation in vitro. Since mesangial cells were identified as the possible target of podocyte-derived Shh (Figure 1), we then investigated the actions of Shh in mesangial cells by using an in vitro system. To this end, human mesangial cells were incubated with different doses of recombinant human Shh for various periods of time. As expected, Shh was able to induce hedgehog downstream Gli1 and Gli2 expression in mesangial cells (Figure 2A). Similarly, Shh also induced Patched 1 (Ptch1) receptor in mesangial cells but did not affect Smoothened (Smo) expression (Supplemental Figure 3). However, Shh had little effect on the expression of Gli1 and Gli2 (Figure 2B) as well as Ptch1 and Smo (Supplemental Figure 3) in mouse podocytes.

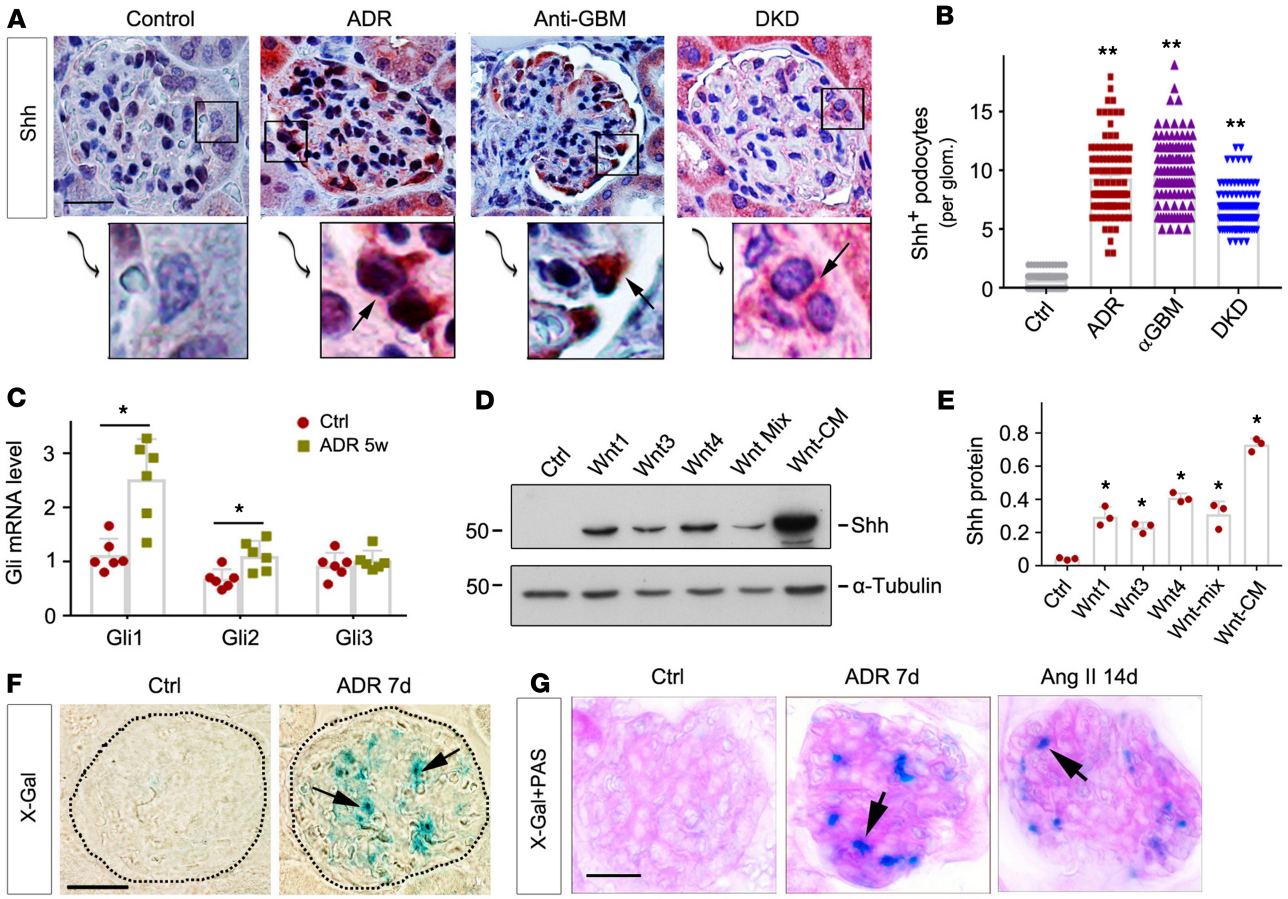

Figure 1. Shh is induced in glomerular podocytes and selectively targets mesangial cells after injury. (**A**) Representative micrographs show that Shh was induced in glomerular podocytes in various models of proteinuric kidney diseases, including adriamycin nephropathy (ADR), anti–glomerular basement membrane glomerulonephritis (anti-GBM), and diabetic kidney disease (DKD). Boxed areas are enlarged and presented below. Arrows indicate positive staining. Scale bar: 25 μm. (**B**) Quantitative determination of Shh$^+$ podocytes in the glomeruli of different models. Shh$^+$ podocytes were counted on 20 glomerular cross sections per mice; 5 mice per group. $^{**}P < 0.01$ versus controls ($n = 5$, Student-Newman-Keuls test). (**C**) Quantitative, real-time PCR (qPCR) analyses reveal that Gli1 and Gli2 mRNA were induced at 5 weeks after ADR administration. $^{*}P < 0.05$ versus shams ($n = 6$, t test). (**D** and **E**) Western blot analyses show that Shh was induced at 48 hours after incubation with various Wnt ligands in cultured podocytes. Cell lysates were immunoblotted with antibodies against Shh and α-tubulin. Wnt mix, a combination of Wnt1, Wnt3, and Wnt4 proteins; Wnt-CM, conditioned media of HKC-8 cells transfected with expression vector pHA-Wnt1 and pHA-Wnt4. Representative Western blot (**D**) and quantitative data (**E**) are shown. $^{*}P < 0.05$ versus controls ($n = 3$, Student-Newman-Keuls test). (**F** and **G**) Identification of the hedgehog-responding cells in the glomeruli after kidney injury using Gli1-LacZ reporter mice. Gli1-LacZ reporter mice were injected with a single dose of ADR or chronic infusion of angiotensin II (Ang II). At 7 days after ADR or 14 days after Ang II, kidney sections were subjected to X-Gal staining. Arrows indicate β-Gal$^+$ cells located at the mesangium. Images with X-Gal staining combined with PAS staining (**G**) are also presented. Dotted lines denote the border of glomerulus. Scale bar: 25 μm.

We observed an appreciable increase in mesangial cell densities after Shh treatment, as illustrated by phase-contrast microscopy (Figure 2C). Cell counting revealed that Shh substantially increased the number of mesangial cells in a time- and dose-dependent manner (Figure 2, D and E), suggesting Shh as a potent mitogen promoting mesangial cell proliferation. Similar results were obtained using a quantitative colorimetric MTT assay (Figure 2, F and G). However, Shh did not affect the growth of podocytes (Figure 2, H and I) or endothelial cells (24). We further assessed the ability of Shh to promote mesangial cells to enter cell cycle and undergo DNA synthesis, which was reflected by BrdU incorporation. As shown in Figure 2J and Supplemental Figure 4, BrdU$^+$ cells were increased in the mesangial cells after incubation with different doses of Shh, compared with the controls.

To elucidate the mechanism underlying Shh's promotion of mesangial cell activation and proliferation, we next assessed the expression of numerous proliferation-related genes. As shown in Figure 2K, proliferating cell nuclear antigen (PCNA), cyclin D1, c-fos, and c-Myc were induced in mesangial cells after incubation with Shh. Meanwhile, Shh also promoted mesangial cell activation, as manifested by the induction of fibronectin, PDGFR-β, and α-smooth muscle actin (α-SMA) (Figure 2, K and L, and Supplemental Figures 4 and 5).

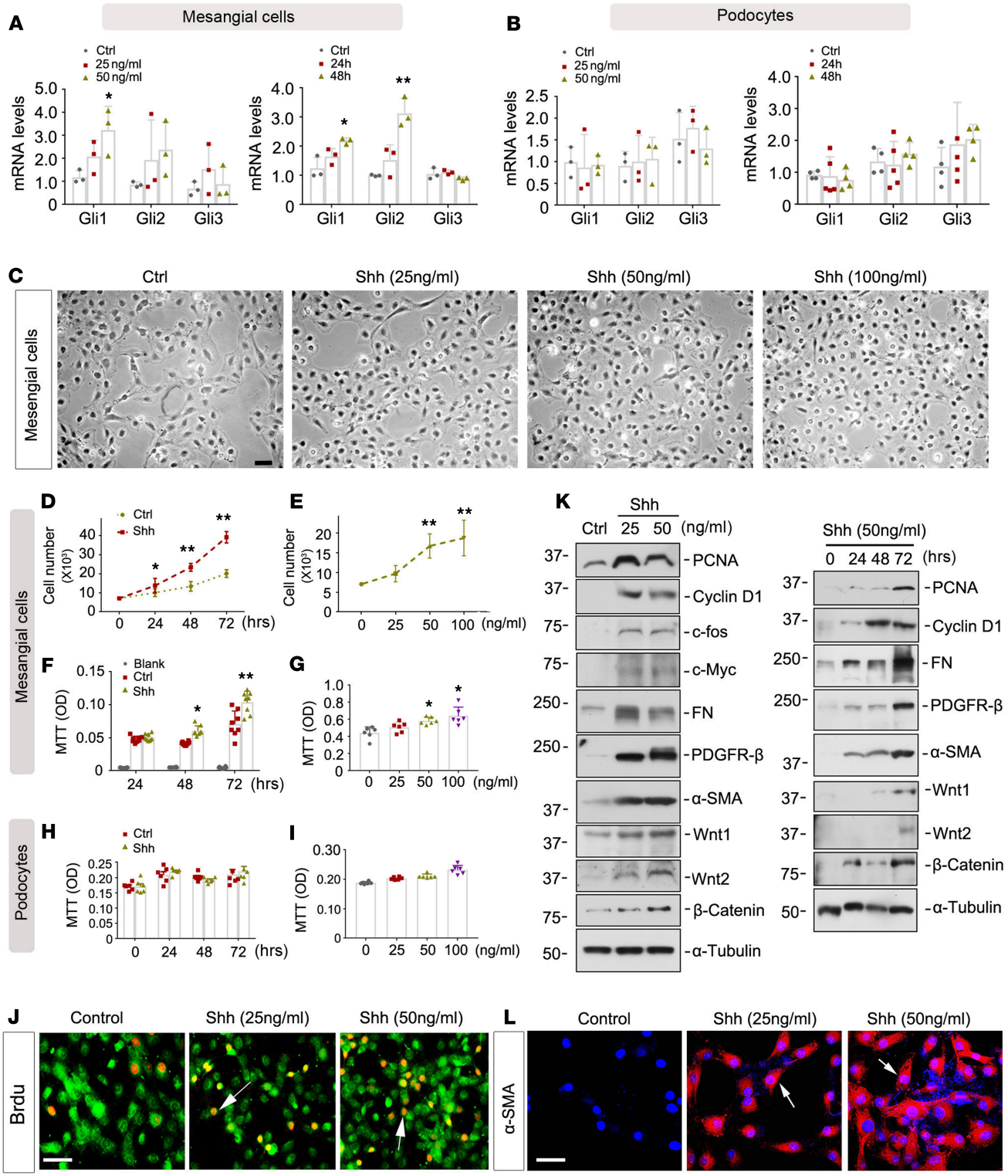

Figure 2. Shh selectively promotes mesangial cell activation and proliferation in vitro. (**A**) qPCR shows that Shh induced Gli1 and Gli2 expression in cultured mesangial cells in a dose-and time-dependent manner. *$P < 0.05$, **$P < 0.01$ versus controls ($n = 3$, Student-Newman-Keuls test). (**B**) Shh did not have a significant effect on Gli1 and Gli2 expression in cultured podocytes ($n = 3$, Student-Newman-Keuls test). (**C**) Representative micrographs show the phase-contrast images of glomerular mesangial cells after incubation with different doses of Shh for 48 hours. Scale bar: 10 μm. (**D** and **E**) Cell counting demonstrates that Shh promoted mesangial cell proliferation in a dose- and time-dependent manner. Glomerular mesangial cells were incubated with a fixed dose of Shh (100 ng/ml) for various periods of time (**D**) or with different concentrations of Shh for 3 days (**E**). Cell numbers ($\times 10^4$ per well) were counted and are presented. *$P < 0.05$, **$P < 0.01$ versus controls ($n = 3$, Student-Newman-Keuls test). (**F** and **G**) Colorimetric MTT assay shows that Shh promoted mesangial cell proliferation in a time- (**F**) and dose-dependent fashion (**G**). *$P < 0.05$, **$P < 0.01$ versus controls ($n = 3$, Student-Newman-Keuls test). (**H** and **I**) Shh did not affect podocyte proliferation, as assessed by MTT assay. (**J**) Representative micrographs show that Shh promoted

mesangial cell DNA synthesis, as demonstrated by BrdU incorporation. Mesangial cells were incubated with 25 and 50 ng/ml Shh for 2 days, respectively. Cells were immunostained with mouse anti-BrdU antibody (red). SYTO-Green was used to visualize the nuclei. Arrows indicate BrdU$^+$ cells. Scale bar: 20 μm. (**K**) Western blots show that Shh induced the expression of numerous proliferation-related genes in cultured mesangial cells. Cell lysates were subjected to Western blot analyses for PCNA, cyclin D1, c-fos, c-Myc, fibronectin (FN), PDGFR-β, α-SMA, Wnt1, Wnt2, β-catenin, and α-tubulin, respectively. (**L**) Representative micrographs show that Shh activated mesangial cells by inducing α-SMA expression after incubation for 2 days. Scale bar: 20 μm.

In addition, Shh also induced Wnt ligands in mesangial cells (Figure 2K), which could further induce Shh expression in podocytes (Figure 1), forming a positive feedback loop.

Shh selectively activates mesangial cells in miniorgan cultured glomeruli ex vivo. To further corroborate the specificity of Shh action on mesangial cells, we used an ex vivo approach by using miniorgan culture of glomeruli. To this end, glomeruli were isolated from normal rat kidneys and incubated with Shh protein. As shown in Figure 3A, transmission electron microscopy showed few changes in the ultrastructure of podocyte foot process and slit diaphragm after Shh treatment, compared with the controls. Consistently, there was little or no difference in the expression of several podocyte-specific proteins, such as nephrin, podocalyxin, α-actinin-4, and Wilms tumor protein 1 (WT1), as illustrated Western blot analyses (Figure 3, B and C). However, Shh induced PDGFR-β, fibronectin, and α-SMA expression in the isolated glomeruli, compared with the controls (Figure 3, D and E), suggesting that Shh specifically promotes mesangial cell activation. Consistently, immunofluorescence staining gave rise to similar results (Figure 3, F–I). Immunostaining for nestin and PDGFR-β revealed a marked mesangial expansion in the cultured glomeruli (Figure 3, H and I). In agreement with Wnt induction (Figure 2), Shh also induced β-catenin expression in glomerular miniorgan culture (Figure 3, D and E). Together, these findings suggest that podocyte-derived Shh selectively targets to mesangial cells and promotes their activation.

Podocyte-specific ablation of Shh uncouples proteinuria with mesangial activation in vivo. To investigate the relevance of Shh to proteinuric CKD in vivo, we next generated conditional knockout mice with podocyte-specific ablation of Shh by using the Cre-LoxP system. Details regarding the breeding, genotyping, and characterization of these mice, designated as Podo-Shh$^{-/-}$ mice, are presented in Supplemental Figure 6. Under physiologic conditions, Podo-Shh$^{-/-}$ mice were phenotypically normal in kidney morphology and function.

We then challenged these Podo-Shh$^{-/-}$ mice with ADR to induce proteinuric CKD (Figure 4A). As shown in Figure 4B, ablation of Shh in podocytes inhibited renal Gli1 expression at 1 week after ADR injection, compared with the age- and sex-matched control littermates. Remarkably, despite the podocyte-specific induction of Shh in this model (Figure 1), ablation of Shh did not affect the severity of albuminuria at different time points after ADR, as shown in Figure 4, C and D. qPCR also confirmed that there was little change in the expression of podocyte-specific proteins, such as nephrin, podocin, CD2AP, podocalyxin, and WT-1, between control and Podo-Shh$^{-/-}$ mice at 1 week after ADR (Figure 4E). The abundance and distribution of nephrin and α-actinin-4 proteins were not affected in Podo-Shh$^{-/-}$ kidneys, compared with the controls (Figure 4F and Supplemental Figure 7A). There was no difference in podocyte ultrastructure and foot process effacement after ADR between the 2 groups (Figure 4F). In a separate experiment, pharmacologic inhibition of Shh signaling by cyclopamine (CPN) also did not affect albuminuria at 4 and 7 days after ADR (Supplemental Figure 7B).

We further analyzed mesangial cell activation in control and Podo-Shh$^{-/-}$ mice at 1 week after ADR. As shown in Figure 4, G and H, loss of Shh in podocytes inhibited the expression of α-SMA but not PDGFR-β. Consistently, double immunostaining confirmed that loss of podocyte-originated Shh inhibited mesangial cell activation (α-SMA) but not abundance (PDGFR-β) in this short period after ADR (Figure 4, I–K). Because of the short duration after ADR, there was no sclerotic lesion in the glomeruli yet as shown by periodic acid–Schiff (PAS) staining and PAS-methenamine (PASM) staining (Figure 4I).

Podocyte-specific ablation of Shh uncouples proteinuria with glomerulosclerosis in vivo. We investigated the role of podocyte-derived Shh in the chronic progression of glomerular diseases. To this end, we examined ADR nephropathy in mice for 5 weeks, a long period when both proteinuria and glomerulosclerosis develop in this model (25). As shown in Figure 5A, albuminuria levels displayed little difference between control and Podo-Shh$^{-/-}$ mice throughout the period of experiment, indicating that podocyte-derived Shh has no effect on podocyte function. Consistently, there was little difference in the mRNA levels of podocyte markers, including nephrin, podocin, CD2AP, and WT1 (Figure 5B). No significant change was found in α-actinin-4 and podocalyxin proteins at 5 weeks after ADR (Figure 5, C and D). Of note, the Shh mRNA level was repressed at 5 weeks in Podo-Shh$^{-/-}$ mice (Supplemental Figure 8A). However, there was no change in renal

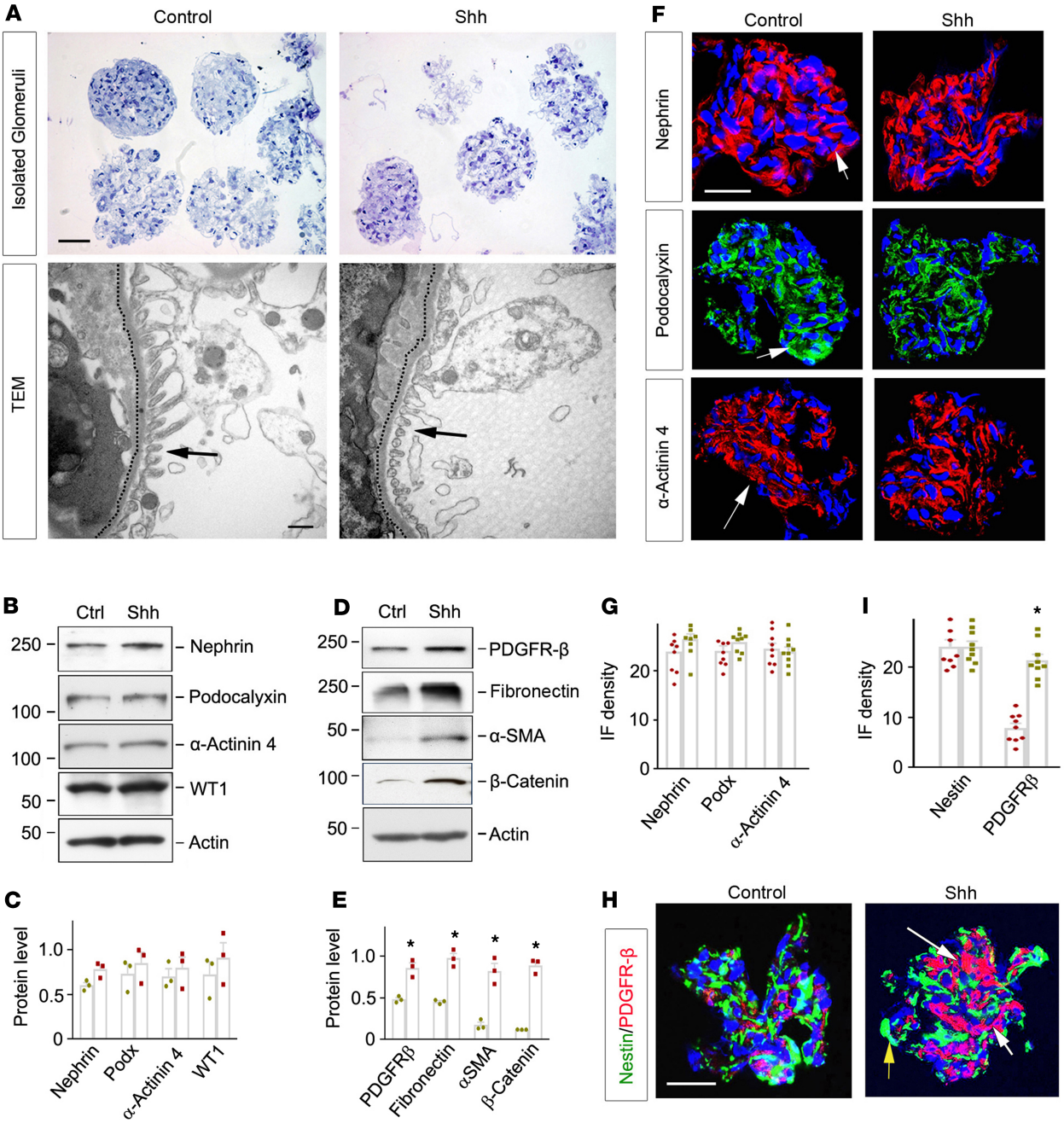

Figure 3. Shh selectively promotes mesangial cell activation in glomerular miniorgan culture ex vivo. (**A**) Representative micrographs show that Shh did not significantly affect podocyte integrity and ultrastructure ex vivo. Isolated glomeruli from normal rats were incubated in the absence or presence of Shh (50 ng/ml) for 24 hours. Transmission electron microscopy (TEM) demonstrates that podocyte foot processes and slit diaphragm were largely preserved after Shh incubation. Arrows indicate slit diaphragm. Dotted lines indicate the boundary of glomerular basement membrane. Scale bar: 25 μm (top); 500 nm (bottom). (**B** and **C**) Western blots show that Shh did not affect the abundance of podocyte-specific proteins, such as nephrin, podocalyxin, α-actinin-4, and WT1, ex vivo. Representative Western blot (**B**) and quantitative data (**C**) are presented (n = 3, t test). (**D** and **E**) Western blots show that Shh induced mesangial cell activation in glomerular miniorgan culture. Isolated glomeruli were incubated with Shh (50 ng/ml) for 24 hours, and glomerular lysates were immunoblotted with antibodies against PDGFR-β, fibronectin, α-SMA, β-catenin, and α-tubulin, respectively. Representative Western blot (**D**) and quantitative data (**E**) are presented. *P < 0.05 versus controls (n = 3, t test). (**F** and **G**) Immunofluorescence staining shows that Shh did not change the expression and localization of podocyte-specific proteins ex vivo. Isolated glomeruli were incubated without or with Shh for 24 hours, and glomerular sections were immunostained for nephrin, podocalyxin, and α-actinin-4 proteins. Representative micrographs (**F**) and quantitation of immunofluorescence (IF) intensity (arbitrary unit) (**G**) are shown. Data were obtained from 3 glomeruli per experiment; 3 independent experiments per group. Arrows indicate positive staining. Scale bar: 20 μm. (**H** and **I**) Double staining shows that Shh selectively promoted mesangial cell activation. Isolated glomeruli were incubated without or with Shh for 24 hours and subjected to double immunostaining for podocyte marker nestin (green) and mesangial cell marker PDGFR-β (red). Representative micrographs (**H**) and quantitation of IF intensity (arbitrary unit) (**I**) are shown. *P < 0.05 versus controls, t test. Data were obtained from 3 glomeruli per experiment; 3 independent experiments per group. White arrows indicate PDGFR-β$^+$ mesangium, whereas yellow arrows denote nestin$^+$ podocytes. Scale bar: 20 μm.

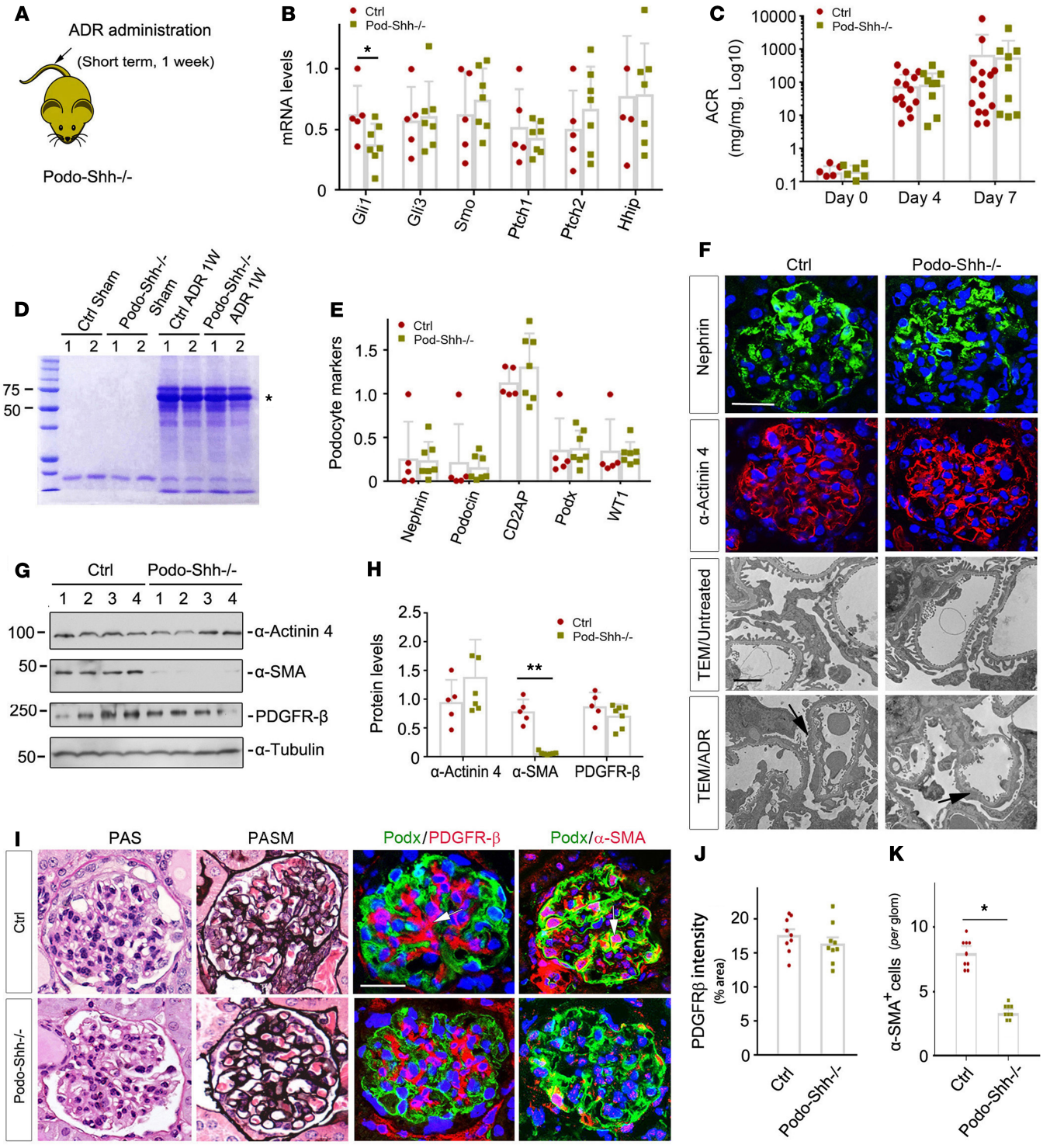

Figure 4. Genetic ablation of podocyte Shh does not affect proteinuria but inhibits mesangial cell activation after injury. (**A**) Generation of conditional knockout mice with podocyte-specific ablation of Shh. (**B**) qPCR reveals that loss of podocyte Shh repressed Gli1 expression at 1 week after ADR injection. *$P < 0.05$ versus controls ($n = 5–7$, t test). (**C**) Podocyte-specific ablation of Shh did not affect albuminuria at day 4 and day 7 after ADR injection ($n = 12–17$). (**D**) SDS-PAGE analysis shows the abundance and composition of urinary proteins in different groups of mice at 1 week after ADR. Urine samples after normalization to creatinine were analyzed on SDS-PAGE. The numbers (1 and 2) indicate each individual animal in a given group. The asterisk indicates the position of albumin. (**E**) qPCR reveals that loss of Shh in podocytes did not affect nephrin, podocin, CD2AP, podocalyxin, and WT1 expression at 1 week after ADR, compared with the controls ($n = 5–7$, t test). (**F**) Representative micrographs show that loss of Shh in podocytes affected neither nephrin and α-actinin-4 expression nor podocyte ultrastructure at 1 week after ADR. Scale bar: 20 μm. Scale bar in transmission electron microscopy (TEM) images: 500 nm. (**G** and **H**) Western blot analyses demonstrate that loss of Shh in podocyte had little effect on α-actinin-4 and PDGFR-β expression but inhibited α-SMA induction at 1 week after ADR. Representative Western blots (**G**) and quantitative data (**H**) are presented. Numbers (1 through 4) indicate each individual animal in a given group. *$P < 0.05$ ($n = 7$, t test). (**I**) Representative

micrographs show that ablation of Shh in podocytes did not affect mesangial abundance but inhibited mesangial activation at 1 week after ADR. Kidney sections were subjected to PAS and PASM staining or double immunofluorescence staining for podocalyxin (green) and PDGFR-β (red) or podocalyxin (green) and α-SMA (red). Arrows indicate positive staining. Scale bar: 20 μm. (**J**) Quantitation of IF intensity (arbitrary unit) of PDGFR-β in the glomeruli of control and podo-Shh$^{-/-}$ mice at 7 days after ADR. (**K**) Quantitation of α-SMA$^+$ cells in the glomeruli of control and podo-Shh$^{-/-}$ mice. *$P < 0.05$ versus controls, *t* test.

function, as assessed by serum creatinine and blood urea nitrogen (BUN), between control and Podo-Shh$^{-/-}$ mice (Supplemental Figure 8, B and C).

Despite the lack of change in proteinuria, we observed a marked difference in glomerular sclerotic lesions between control and Podo-Shh$^{-/-}$ mice at 5 weeks after ADR. As shown in Figure 5E, loss of Shh in podocytes inhibited the mRNA expression of several fibrosis-related genes, such as α-SMA, fibroblast-specific protein 1 (Fsp1), collagen I, and collagen III. Likewise, fibronectin, β-catenin, PDGFR-β, and α-SMA protein levels were decreased in Podo-Shh$^{-/-}$ mice at 5 weeks after ADR, compared with the controls (Figure 5, F–J, and Supplemental Figure 9). Glomerulosclerosis was evident in kidneys sections of control mice after PAS and Masson's trichrome staining (MTS), which was mitigated in Podo-Shh$^{-/-}$ mice (Figure 5, J and K).

Pharmacologic inhibition of Shh signaling selectively mitigates glomerulosclerosis. To validate the role of Shh signaling in glomerular diseases in vivo, we used a pharmacological approach by inhibiting Shh signaling with CPN in ADR nephropathy. As presented in Figure 6A, CPN was given immediately after ADR for 5 weeks. Inhibition of Shh signaling by CPN was able to repress renal Gli1 expression (Figure 6B). However, treatment with CPN for 5 weeks exhibited little effect on albuminuria (Figure 6C) and renal expression of nephrin, podocin, CD2AP, and WT1 (Figure 6D). ADR caused marked reduction of α-actinin-4 expression, which was not affected by CPN treatment (Figure 6, E–H).

Consistent with the findings in the genetic Podo-Shh$^{-/-}$ model, pharmacologic inhibition of Shh signaling by CPN was able to abolish the induction of several fibrosis-related proteins, such as PDGFR-β, fibronectin, α-SMA, and β-catenin (Figure 6, I–K). Immunostaining also revealed that CPN reduced PDGFR-β and α-SMA expression specifically in the mesangial area at 5 weeks after ADR (Figure 6, L and M). Of interest, CPN appeared not to inhibit α-SMA expression in podocytes (Figure 6L, yellow arrows). Consistently, MTS exhibited a marked reduction of collagen deposition by CPN in the glomeruli (Figure 6, L and N).

Blockade of Shh signaling attenuates glomerulosclerosis in DKD. To generalize the finding of Shh on glomerulosclerosis, we also investigated the effect of Shh inhibition on DKD, the most common form of CKD (26, 27). To this end, we used *db/db* mice, the classic model of type 2 diabetes characterized by obesity and dyslipidemia due to deficiency of leptin receptor (28). At the age of 24 weeks, *db/db* mice were administered with CPN or vehicle for 2 weeks. As shown in Figure 7, A and B, CPN neither ameliorated albuminuria nor affected the expression of nephrin, podocin, and CD2AP in this model. Of note, CPN also did not affect blood glucose and serum creatinine levels in this model (Supplemental Figure 10).

Interestingly, administration of CPN for 2 weeks inhibited renal expression of several fibrosis-related genes, such as fibronectin, collagen I, and α-SMA in *db/db* mice (Figure 7C). Although CPN did not affect podocyte-specific α-actinin-4 protein abundance, it repressed PDGFR-β, β-catenin, and α-SMA in the kidneys of mice with DKD (Figure 7, D and E). Double immunofluorescence staining confirmed that CPN selectively inhibited PDGFR-β and α-SMA expression in the glomerular mesangial area, whereas it had little effect on nephrin expression and distribution (Figure 7, F–I). Furthermore, staining with PAS, PASM, and MTS demonstrated that CPN alleviated glomerulosclerotic lesions in the kidneys of *db/db* mice (Figure 7, J and K).

Shh is correlated with glomerulosclerosis in human CKD. To establish the clinical relevance of Shh to human CKD, we investigated its expression in human kidney biopsies from patients diagnosed with various glomerular diseases. As shown in Figure 8A, immunohistochemical staining revealed that Shh protein was barely detectable in normal human glomeruli (3 cases tested). However, Shh protein was clearly induced in the glomeruli of diseased kidneys in all 10 biopsy specimens from patients with various glomerular diseases, including IgA nephropathy, FSGS, and membranous nephritis (Supplemental Table 1). Shh protein was predominantly localized in podocyte in human diseased glomeruli (Figure 8A, arrows), whereas glomerular mesangial cells were virtually negative for Shh staining. In patients with proteinuric CKD, circulating Shh levels were elevated in sera, compared with healthy subjects (Figure 8B)

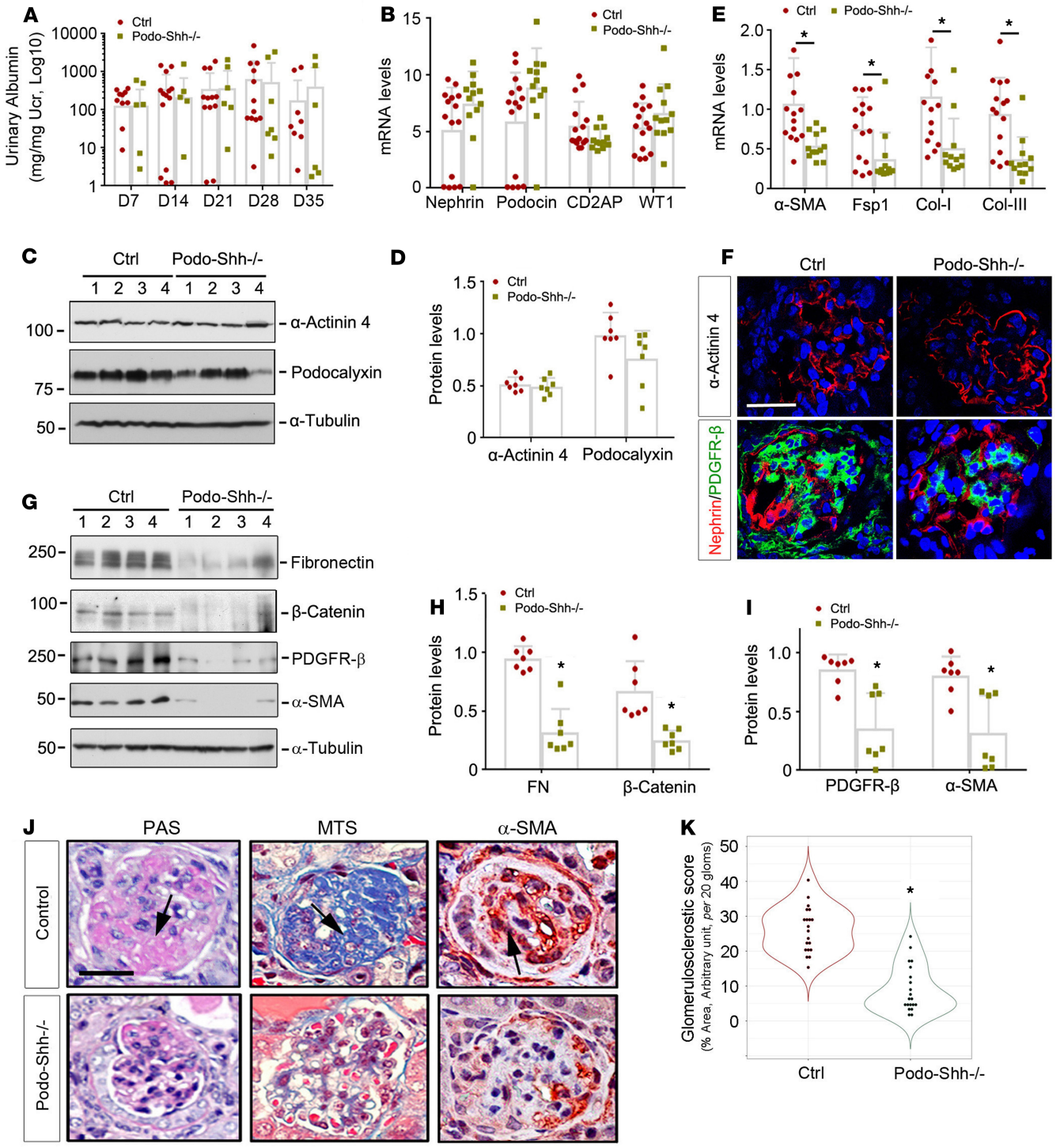

Figure 5. Podocyte-specific deletion of Shh decouples proteinuria from glomerulosclerosis at 5 weeks after ADR injection. (**A**) Podocyte-specific ablation of Shh did not affect albuminuria at different time points after ADR injection (n = 5–14). Urines were collected from mice at 1, 2, 3, 4, and 5 weeks after ADR injection. (**B**) qPCR analyses revealed that podocyte-specific loss of Shh did not affect nephrin, podocin, CD2AP, and WT1 expression at 5 weeks after ADR injection (n = 13–15). (**C** and **D**) Ablation of Shh did not affect podocyte-specific protein expression. Representative Western blots (**C**) and quantitative data (**D**) showed the expression of α-actinin-4 and podocalyxin at 5 weeks after ADR. (**E**) qPCR analyses revealed that loss of podocyte Shh repressed α-SMA, FSP-1, collagen type I, and collagen type III expression at 5 weeks after ADR injection. *P < 0.05 versus controls (n = 13–15, t test). (**F**) Representative micrographs showed the expression of actinin-4, nephrin (red), and PDGFR-β (green) in the glomeruli of control and Podo-Shh$^{-/-}$ mice. Scale bar: 25 μm. (**G**–**I**) Podocyte-specific ablation of Shh repressed protein expression of fibronectin, α-SMA, β-catenin, and PDGFR-β at 5 weeks after ADR injection. Representative Western blots (**G**) and quantitative data (**H** and **I**) are presented. Numbers (1 through 4) indicate each individual animal in a given group. *P < 0.05 versus controls (n = 10, t test). (**J**) Representative micrographs showed a decreased glomerulosclerotic lesion and reduced α-SMA expression at 5 weeks after ADR injection in Podo-Shh$^{-/-}$ mice, compared with controls. Glomerulosclerotic lesions were assessed by PAS and Masson's trichrome staining (MTS). Arrows indicate positive staining. Scale bar: 20 μm. (**K**) Quantitative determination of glomerulosclerotic score. The percentage of sclerotic area was assessed in 20 glomeruli. *P < 0.05 versus controls, t test.

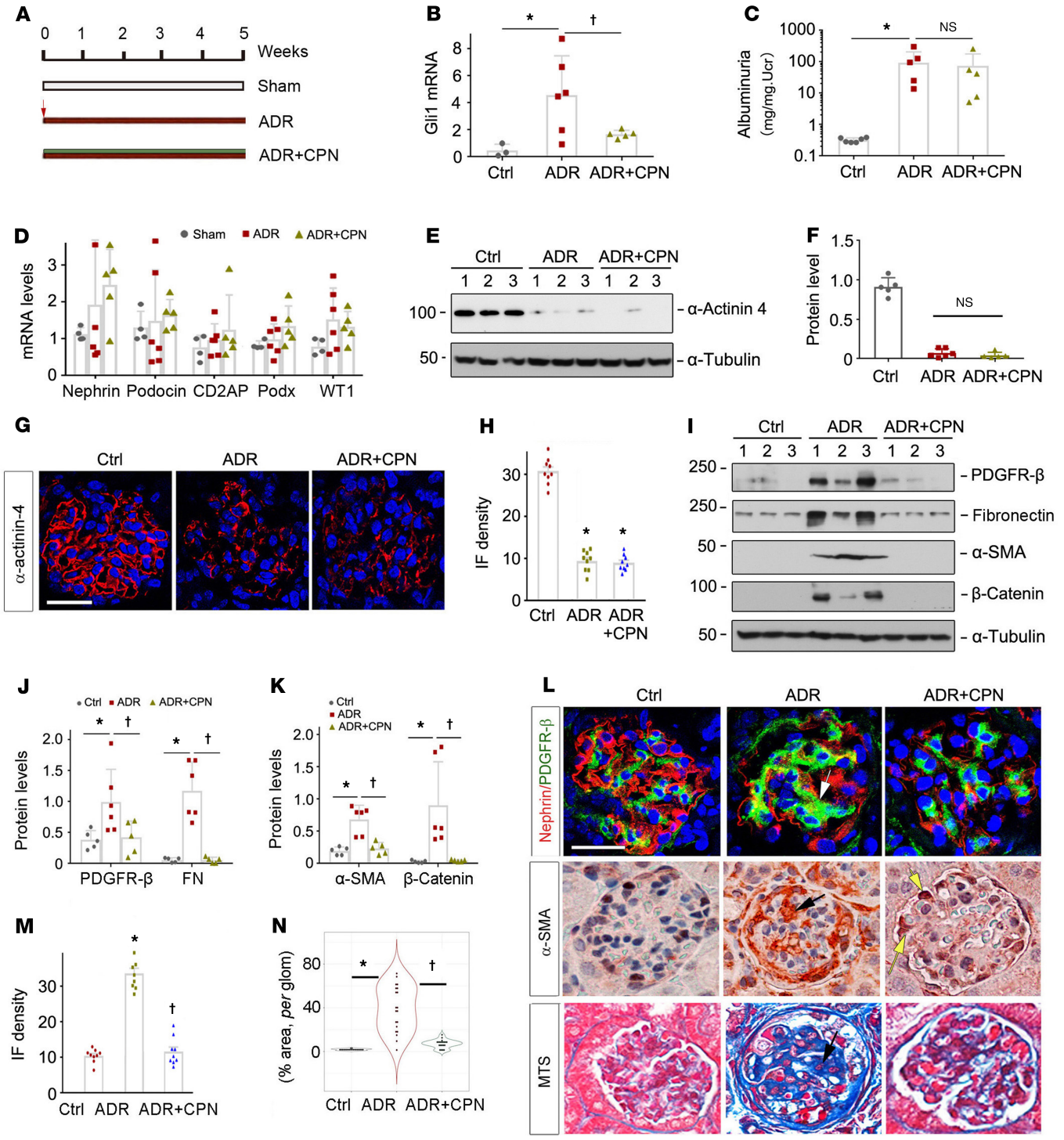

Figure 6. Pharmacologic inhibition of Shh signaling decouples proteinuria from glomerulosclerosis. (**A**) Experimental design. Red arrow, ADR injection. Green bar, CPN treatment. (**B**) qPCR analyses reveal that pharmacologic inhibition of Shh signaling repressed Gli1 expression at 5 weeks after ADR injection, compared with the vehicles. *$P < 0.05$ versus controls, †$P < 0.05$ versus ADR alone (n = 5–6, Student-Newman-Keuls test). (**C**) Inhibition of Shh signaling by CPN did not affect albuminuria at 5 weeks after ADR. *$P < 0.05$ (n = 5–6, Student-Newman-Keuls test). (**D**) qPCR analyses revealed that inhibition of Shh signaling by CPN did not affect nephrin, podocin, CD2AP, podocalyxin, and WT1 expression at 5 weeks after ADR injection, compared with the vehicles (n = 4–5, Student-Newman-Keuls test). (**E** and **F**) Western blot analyses showed that CPN did not affect α-actinin-4 expression at 5 weeks after ADR injection. Representative Western blot (**E**) and quantitative data (**F**) are presented (n = 5–6). (**G** and **H**) Representative micrographs and quantitation of IF intensity (arbitrary unit) showed α-actinin-4 expression and localization in the glomeruli of mice after various treatments as indicated. Scale bar: 20 μm. *$P < 0.05$ versus controls, Student-Newman-Keuls test. (**I**–**K**) Western blot assays showed that CPN inhibited the expression of fibrosis-related genes, including PDGFR-β, fibronectin, α-SMA, and β-catenin at 5 weeks after ADR injection. Representative Western blot (**I**) and quantitative data (**J** and **K**) are presented. *$P < 0.05$ versus controls, †$P < 0.05$ versus ADR alone (n = 5–6, Student-Newman-Keuls test). (**L**) Representative micrographs showed that CPN did not preserve podocyte integrity but inhibited mesangial activation and glomerulosclerosis.

Kidney sections were immunostained for nephrin (red), PDGFR-β (green), and α-SMA or subjected to Masson's trichrome staining. Arrows indicate positive staining. The yellow arrows denotes α-SMA$^+$ podocytes. Scale bar: 25 μm. (**M**) Quantitation of IF intensity (arbitrary unit) of PDGFR-β in the glomeruli at 5 weeks after ADR in the absence or presence of CPN. *$P < 0.05$ versus controls, †$P < 0.05$ versus ADR alone, Student-Newman-Keuls test. (**N**) Quantitative determination of glomerulosclerotic score. The percentage of sclerotic area was assessed in 20 glomeruli. *$P < 0.05$ versus controls, †$P < 0.05$ versus ADR alone, Student-Newman-Keuls test.

(Supplemental Table 2). Of note, Shh protein in urine samples was extremely low or undetectable (data not shown). Consistent with animal models, serum Shh was correlated with neither total urinary protein nor albuminuria levels, as shown in Figure 8, C and D. However, circulating Shh levels were associated with glomerular histologic lesions, such as adhesion to Bowman's capsule and glomerulosclerosis in CKD patients (Figure 8E). Figure 8F shows representative micrographs of the glomerulosclerotic lesions revealed by MTS and PASM staining in 2 patients with different levels of serum Shh, suggesting that Shh is associated with glomerulosclerosis, but not proteinuria, in patients as well. Taken together, we conclude that Shh plays a crucial role in mediating podocyte-mesangial crosstalk (Figure 8G) and mechanistically links proteinuria to glomerulosclerosis.

Discussion

Proteinuria and glomerulosclerosis are two principal pathologic features of a wide variety of glomerular diseases (29). In this study, we present evidence for an intrinsic connection between these two processes through a podocyte-mesangial communication mediated by Shh ligand. This conclusion is supported by several lines of evidence, including that (a) Shh is specifically induced in the glomerular podocytes in various animal models of CKD; (b) Shh selectively targets glomerular mesangial cells and induces their activation and proliferation in vitro, in vivo, and ex vivo; (c) podocyte-specific ablation of Shh uncouples mesangial cell activation and glomerulosclerosis from proteinuria after injury; (d) pharmacologic inhibition of Shh signaling by CPN selectively suppresses mesangial activation and ameliorates glomerulosclerosis in ADR nephropathy and DKD; and (e) Shh is also induced in the glomerular podocytes in patients with proteinuric CKD and its circulating levels are correlated with glomerulosclerotic lesions. Taken together, these studies have identified Shh as the long-sought mediator that couples proteinuria to glomerulosclerosis in the pathogenesis of glomerular diseases. To the best of our knowledge, the present study represents the first report that links podocyte injury to mesangial activation, thereby providing mechanistic insights into the development and progression of proteinuric CKD.

Proteinuria, as the clinical manifestation of an impaired glomerular filtration barrier, is an early marker in the pathogenesis of glomerular disease. Extensive studies have shown that podocyte injury often causes the destruction of the fine ultrastructure of podocyte foot processes and slit diaphragm and plays a fundamental role in the onset of proteinuria (5, 30, 31). Activation of several key signal pathways, such as Wnt/β-catenin, TGF-β1, and the renin-angiotensin system has been implicated in causing podocyte dysfunction, leading to a defective glomerular filtration and proteinuria (32–36). Consistently, strategies to inhibit this signaling protect podocyte integrity and mitigate proteinuria (25, 37). In this study, we show that podocyte injury is also accompanied by Shh induction in a wide range of proteinuric CKD, including DKD, ADR nephropathy, anti-GBM, IgA nephropathy, and FSGS, underscoring that podocyte-specific upregulation of Shh ligand is a common pathologic feature of many proteinuric CKD. Surprisingly, such an induction of Shh does not affect podocyte integrity and function, as Shh neither impairs podocyte slit diaphragm and fine ultrastructure nor changes the expression of podocyte-specific proteins, such as nephrin, podocalyxin, α-actinin-4, and WT1 ex vivo (Figure 3). Accordingly, podocyte-specific ablation of Shh in mice does not affect proteinuria after ADR injury (Figures 4 and 5). These findings are also substantiated by the observation that podocytes do not respond to hedgehog stimulation in the Gli1-LacZ–knockin reporter mice after glomerular injury (Figure 1). Although more studies in other proteinuric CKD models are needed, the present study indicates that Shh is a marker of podocyte injury, which itself has no real influence on podocyte dysfunction and the severity of proteinuria. In this regard, unlike TGF-β1, Wnts, and the renin-angiotensin system, Shh is quite unique in that it does not exert autocrine actions in podocytes.

The most interesting finding of the present study is that Shh connects podocyte damage to mesangial activation and glomerulosclerosis by mediating a unique podocyte-mesangial communication via a paracrine fashion. This conclusion is supported by the observations that Shh is able to promote mesangial cell activation in different model systems, in vitro, ex vivo, and in vivo, but does not

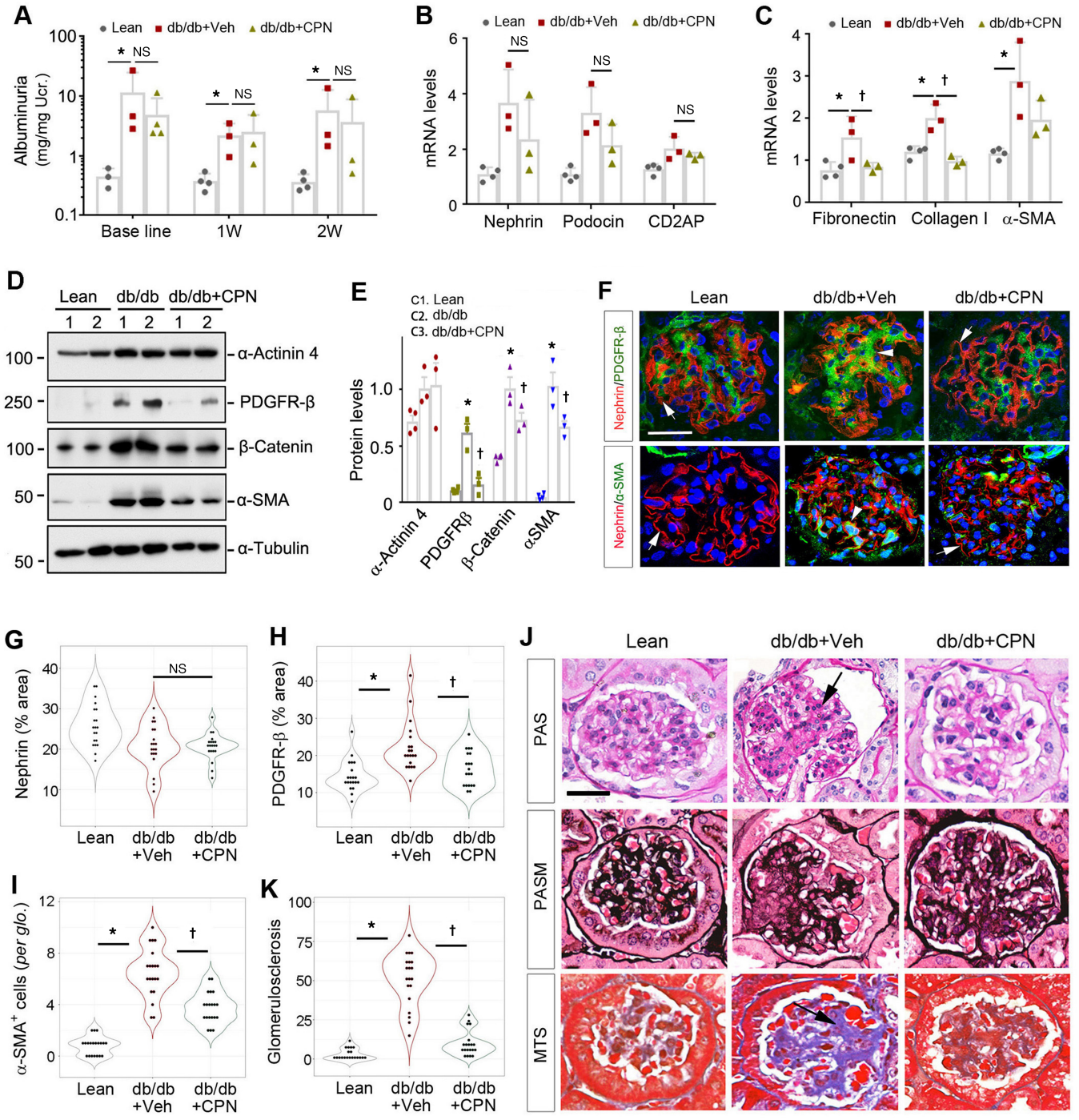

Figure 7. Blockade Shh signaling attenuates glomerulosclerosis in diabetic kidney disease. (**A**) Urinary albumin levels of *db/db* mice at different time points after CPN treatment. *$P < 0.05$ versus lean mice ($n = 3–4$, Student-Newman-Keuls test). (**B** and **C**) qPCR showed that CPN did not significantly affect podocyte-specific genes, such as nephrin, podocin, and CD2AP (**B**) but inhibited numerous fibrosis-related genes, including fibronectin, collagen I, and α-SMA (**C**). *$P < 0.05$ versus lean mice; †$P < 0.05$ versus vehicle ($n = 3–4$, Student-Newman-Keuls test). (**D** and **E**) Western blot analysis showed that CPN has little effect on podocyte-specific α-actinin-4 expression in *db/db* mice, but it inhibited α-SMA, PDGFR-β, and β-catenin expression at 2 weeks after CPN treatment. Representative Western blot (**D**) and quantitative data (**E**) are presented. *$P < 0.05$ versus lean mice, †$P < 0.05$ versus vehicle, Student-Newman-Keuls test. (**F**) Representative micrographs reveal that CPN inhibited glomerular PDGFR-β and α-SMA expression but did not affect nephrin. Arrows indicate nephrin expression, while arrowheads denote PDGFR-β$^+$ and α-SMA$^+$ staining. Scale bar: 25 μm. (**G–I**) Quantitative determination of nephrin (**G**), PDGFR-β (**H**), and α-SMA (**I**) staining in the glomeruli of different groups of mice as indicated. *$P < 0.05$ versus lean mice; †$P < 0.05$ versus vehicle, Student-Newman-Keuls test. (**J**) Representative micrographs revealed that CPN attenuated glomerulosclerosis in *db/db* mice. Kidney sections were subjected to periodic acid–Schiff (PAS), PAS-methenamine (PASM), and Mason's trichrome staining (MTS), respectively. (**K**) Quantitative determination of glomerulosclerosis in different groups of mice as indicated. *$P < 0.05$ versus lean mice; †$P < 0.05$ versus vehicle, Student-Newman-Keuls test.

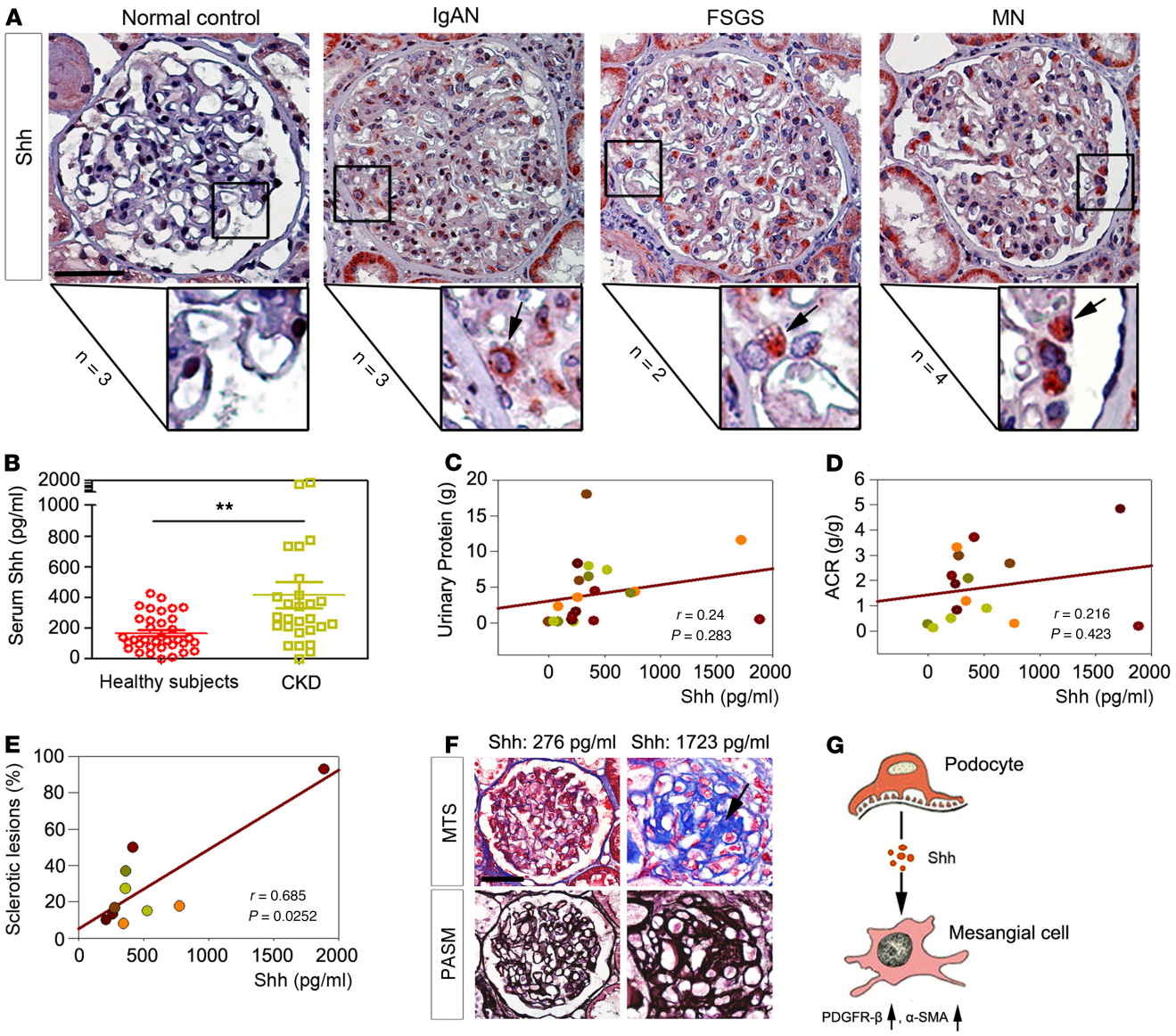

Figure 8. Podocyte-specific induction of Shh is associated with glomerulosclerosis in humans. (**A**) Representative immunohistochemical staining showed a podocyte-specific induction of Shh in human biopsies from various proteinuric CKD, such as IgA nephropathy (IgAN), focal and segmental glomerulosclerosis (FSGS), and membranous nephritis (MN), compared with the healthy controls. Boxed areas are enlarged and presented. Arrows in the enlarged boxes indicate Shh$^+$ podocyte. Scale bar: 50 μm. (**B**) Serum Shh levels in CKD patients diagnosed with different glomerular diseases, compared with healthy adults. $^{**}P < 0.01$ (n = 27–35, t test). (**C**–**E**) Pearson's correlation analyses revealed that Shh has no correlation with proteinuria (**C**) (n = 22) and albuminuria (**D**) (n = 16) levels, but it is closely correlated with the extent of glomerulosclerosis (**E**) (n = 9). (**F**) Representative micrographs of MTS and PASM staining show collagen deposition in the glomeruli of CKD patients with different levels of serum Shh. The serum Shh levels are presented on the top of representative micrographs. Arrow indicates collagen deposition in human kidney biopsies. (**G**) The schematic diagram shows that Shh couples podocyte injury to mesangial activation and glomerulosclerosis.

affect the proliferation of podocytes (Figure 2) or endothelial cells (24). Furthermore, genetic ablation or pharmacologic inhibition of Shh decouples podocyte injury from glomerulosclerosis. Although it has been speculated for a long time that proteinuria and glomerulosclerosis are somehow connected mechanistically, the mediator responsible for such a connection remained elusive. In this context, the present study is quite significant in that it clearly establishes the podocyte-derived Shh as the mediator that orchestrates podocyte-mesangial communication.

Shh, as a morphogen, plays an especial role in mediating intercellular communication via a paracrine mechanism (14). Shh transmits its signaling through binding to the receptor Ptch1, which results in the derepression of Smo. Activated Smo then moves from an intracellular vesicle to the cell membrane,

where it activates the Gli family of transcription factors in Shh-responding cells (14, 38, 39). We previously reported that tubule-derived Shh selectively targets interstitial fibroblasts and induces their activation in CKD, leading to renal fibrosis (16, 17). Similar to its role in the tubulointerstitial compartment, we show here that Shh induces mesangial cell activation in the glomeruli. Therefore, Shh in different renal compartments (podocyte and tubular epithelium) confers similar actions by activating mesangial cells and fibroblasts, respectively. It should be pointed out that podocyte-mesangial communication is quite unique in that podocytes may physically contact mesangial cells directly without the barricade of the GBM (40), making it easy to crosstalk via a paracrine fashion. Notably, podocyte-mesangial communication is most likely to be reciprocal and bidirectional, as podocyte-derived Shh induces Wnt ligands in mesangial cells (Figure 2), which in turn can target podocytes and induce podocyte injury (23, 32), thereby creating a vicious cycle.

The results presented in this study appear to have clinical relevance to human CKD as well. Podocyte induction of Shh is a common finding in human kidney biopsies from patients with various glomerular diseases, including IgA nephropathy, FSGS, and membranous nephropathy. The circulating levels of Shh are closely associated with glomerular sclerotic lesions but not with proteinuria (Figure 8), suggesting that Shh may serve as a surrogate biomarker predicting glomerular sclerotic lesions. It should be noted that the clinical data presented in this study may have its limitation because of small sample sizes. Nevertheless, it provides a proof of principle that Shh links podocyte injury to glomerulosclerosis in humans. Further clinical studies using large sample sizes are warranted in the future. It is worthwhile to point out that, in the advanced stage of CKD when progressive loss of podocytes occurs (6, 41), the overall production of Shh by glomerular podocytes could be decreased.

In summary, we herein demonstrate that Shh is the long-sought mediator that connects podocyte injury with mesangial activation, thereby mechanistically coupling proteinuria to glomerulosclerosis. We show that one can decouple podocyte damage from glomerulosclerotic lesions by targeted inhibition of Shh signaling. Although more studies are needed, these findings provide potentially novel insights into the mechanism linking proteinuria and glomerulosclerosis and suggest Shh signaling as a therapeutic target for ameliorating glomerulosclerosis in clinical setting.

Methods

Animal models. The mouse model of podocyte injury and proteinuria was established by intravenous injection of ADR as described previously (23). Male BALB/c mice weighing 20–22 g and 24-week-old *db/db* mice were obtained from the Envigo. For pharmacologic inhibition experiments, CPN was intraperitoneally injected daily at a dose of 5 mg/kg body weight after ADR or 2 weeks before sacrifice in *db/db* mice. CPN was complexed with 2-hydroxypropyl-β-cyclodextrin (HBC; MilliporeSigma). A CPN/HBC stock solution was prepared by suspending 1 mg CPN in 1 ml 45% HBC in sterile PBS and stirring at 65°C for 60 minutes. Three groups of BALB/c mice were used: (a) sham control (n = 5–6), (b) ADR mice injected with vehicle (n = 6), and (c) ADR mice treated with CPN (n = 6). ADR (doxorubicin hydrochloride; MilliporeSigma) was administered by a single intravenous injection at 10 mg/kg body weight. At 1 and 5 weeks after ADR injection, all mice were euthanized. At 2 weeks after CPN injection, *db/db* mice were killed. Urine, blood, and kidney tissues were collected for various analyses.

Mouse genetic models. The Gli1-LacZ reporter mice, which harbor a β-Gal–knockin mutation that also abolishes endogenous *Gli1* gene function, were obtained from The Jackson Laboratories (stock no. 008211). All animals were born normally at the expected Mendelian frequency, and they were normal in size and did not display any gross physical or behavioral abnormalities.

Homozygous *Shh*-floxed mice (C57BL/6J background) were also purchased from The Jackson Laboratories (stock no. 004293). Transgenic mice expressing Cre recombinase under the control of a 2.5-kb fragment of the human podocin promoter have been described previously (23). By mating Shh-floxed mice with podocin-Cre–transgenic mice, conditional knockout mice in which the *Shh* gene was specifically disrupted in podocytes (genotype $Shh^{fl/fl}$, $Cre^{+/-}$) were created. These mice were crossbred with homozygous Shh-floxed mice (genotype $Shh^{fl/fl}$) to generate offspring with 50% podocin-$Shh^{-/-}$ mice and 50% control mice (podocin-$Shh^{+/+}$) within the same litters. A routine PCR protocol was used for genotyping of tail DNA samples with the following primer pairs: Cre transgene, 5′-AGGTGTAGAGAAGGCACTTAGC-3′ and 5′-CTAATCGCCATCTTCCAGCAGG-3′, which generated a 411-bp fragment; and Shh genotyping, 5′-ATGCTGGCTCGCCTGGCTGTGGAA-3′ and 5′-GAAGAGATCAAGGCAAGCTCTGGC-3′, which yielded 483-bp band for the floxed alleles.

Human kidney biopsy specimens and serum samples. Human kidney specimens were obtained from diagnostic renal biopsies performed at two centers in China, the Affiliated Hospital of Nanjing University of Chinese Medicine and Nanfang Hospital, Southern Medical University. Nontumor kidney tissues from the patients who had renal cell carcinoma and underwent nephrectomy were used as the normal controls. Paraffin-embedded human kidney biopsy sections (2.5-μm thickness) were prepared using a routine procedure. The serum samples were obtained from the Affiliated Hospital of Nanjing University of Chinese Medicine.

Cell culture and treatment. Mouse podocytes were described previously (22). Human mesangial cells were provided by Chuanyue Wu (University of Pittsburgh, Pittsburgh, Pennsylvania, USA). The human kidney proximal tubular cell line (HKC-8) was provided by L. Racusen of the Johns Hopkins University (Baltimore, Maryland, USA). The Wnts-enriched conditioned medium was prepared by transfecting HKC-8 cells with multiple Wnt expression vectors, as reported previously (42). Podocytes were transfected with different Wnts-expressing vectors by Lipofectamine 2000 (Invitrogen) according to the manufacturer's protocol. Whole-cell lysates were prepared and subjected to Western blot analyses.

Glomerular miniorgan culture. Glomeruli were isolated using the differential sieving technique from male Sprague-Dawley rats (Envigo). Briefly, kidneys were excised and pressed with a spatula through stainless steel screens through differential sieves (60, 100, and 200 meshes) and washed with cold PBS/1% BSA. The glomeruli were suspended in PBS/1% BSA. After centrifugation at 200 *g* for 10 minutes, glomeruli were collected for cultivation. The purity of glomeruli was about 95% using this approach. Isolated glomeruli were cultured in RPMI1640/10% FBS medium at 37°C on noncoated 6-well plates in the absence or presence of recombinant Shh protein (1324-WN-010; R&D Systems) for further analyses.

Determination of albuminuria, serum creatinine, BUN, and blood glucose. Urine albumin was measured by using a mouse Albumin ELISA Quantitation Kit according to the manufacturer's protocol (Bethyl Laboratories Inc.). Urine creatinine was determined by a routine procedure as described previously (22). Urinary albumin was standardized to urine creatinine and expressed as milligrams per milligram urinary creatinine. Serum creatinine and BUN levels were determined by using QuantiChrom creatinine and BUN assay kits, according to the protocols specified by the manufacturer (BioAssay Systems). Levels of serum creatinine and BUN were expressed as milligrams per 100 ml (dl). Blood glucose levels were checked by using the Glucose Level Monitoring Device (Accu-Chek).

Shh ELISA. The Shh human ELISA kit was purchased from Abcam (ab100639; Abcam). This assay used an antibody specific for human Shh coated on a 96-well plate. Standards and samples were pipetted into the wells, and Shh present in a sample was bound to the wells by the immobilized antibody. The wells were washed and biotinylated anti-human Shh antibody was added. After washing away unbound biotinylated antibody, HRP-conjugated streptavidin was pipetted to the wells. After the wells were washed again, TMB substrate solution was added to the wells and color developed in proportion to the amount of Shh bound. The stop solution changed the color from blue to yellow, and the intensity of the color was measured at 450 nm.

Cell proliferation assay. Cell proliferation was assessed by two approaches: cell counting and MTT assay. Cell numbers were counted by using a hemocytometer. Cell proliferation was also determined quantitatively by an MTT assay. Briefly, podocytes and mesangial cells were seeded into 96-well plates at a density of 1×10^3/well. After adherence of cells, the cultures were changed to the serum-free medium and incubated for 24 hours followed by treatment with or without Shh at different concentrations for various periods of time. MTT (5 mg/ml) was added to the medium at 10 μl/well followed by incubation at 37°C for 4 hours. After the medium was removed, cells were lysed with 100 μl dimethyl sulfoxide. Absorbance of each well was measured by a microplate reader at 490-nm wavelength.

BrdU incorporation assay. The effect of Shh on human mesangial cell DNA synthesis was evaluated by BrdU incorporation. Briefly, cells were seeded onto 24-well plates and treated with various concentrations of Shh for 48 hours, and then they were pulsed with BrdU (10 mM) for 24 hours. Cells were fixed with ice-cold 70% ethanol for 20 minutes, and DNA was denatured by incubation with 2.5 *N* HCL for 20 minutes followed by neutralization with 0.1 M boric acid. Endogenous peroxidase activity was quenched by incubating the cells with 3% H_2O_2 in PBS for 20 minutes, and nonspecific binding was blocked by incubating the cells with 10% donkey serum for 10 minutes at room temperature. Incorporated BrdU was detected with a mouse monoclonal anti-BrdU antibody (B2531; MilliporeSigma) followed by incubation with cyanine Cy3-conjugated, affinity-purified secondary antibody (Jackson ImmunoResearch Laboratories). Stained cells were mounted with VectaShield anti-fade mounting media (Vector Laboratories) by using SYTO-Green (S34854;

Thermo Fisher) to visualize the nuclei. Stained samples were viewed under an Eclipse E600 epifluorescence microscope equipped with a digital camera (Nikon).

Reverse transcriptase and real-time PCR. Total RNA isolation and qPCR were carried out by the procedures described previously (22). Briefly, the first-strand cDNA synthesis was carried out by using a Reverse Transcription System kit (Promega) according to the manufacturer's instructions. qPCR was performed on ABI PRISM 7000 Sequence Detection System (Applied Biosystems). The PCR reaction mixture in a 25-μl volume contained 12.5 μl 2× SYBR Green PCR Master Mix (Applied Biosystems), 5 μl diluted reverse transcriptase product (1:10), and 0.5 μM sense and antisense primer sets. The PCR reaction was run using standard protocols. After sequential incubations at 50°C for 2 minutes and 95°C for 10 minutes, respectively, the amplification protocol consisted of 40 cycles of denaturing at 95°C for 15 seconds and annealing and extension at 60°C for 60 seconds. The standard curve was made from series dilutions of template cDNA. The mRNA levels of various genes were calculated after normalizing with β-actin. Primer sequences used for amplifications are presented in Supplemental Table 3.

Western blot analysis. Kidney tissues were lysed with radioimmunoprecipitation assay buffer containing 1% NP-40, 0.1% SDS, 100 μg/ml PMSF, 1% protease inhibitor cocktail, and 1% phosphatase I and II inhibitor cocktail (MilliporeSigma) in PBS on ice. The supernatants were collected after centrifugation at 13,000 *g* at 4°C for 15 minutes. Protein expression was analyzed by Western blot analysis as described previously (22). The primary antibodies used were as follows: anti-Shh (sc-9024), anti-PCNA (sc-56), anti-c-fos (sc-52), anti-c-Myc (sc-764), anti-WT1 (sc-7385), and anti-PDGFR-β (sc-432) (Santa Cruz Biotechnology); anti-β-catenin (610154; BD Transduction Laboratories); anti-Wnt1 (ab15251) and anti-Wnt2 (ab109222) (Abcam); anti-cyclin D1 (RB-9041-P0; Neomarkers); anti-nephrin (20R-NP002; Fitzgerald Industries International); anti-podocalyxin (MAB1556, R&D Systems); anti-α-actinin 4 (ALX-210–356-c050; Enzo Life Sciences); anti-α-SMA (A2547), anti-fibronectin (F3648), and anti-α-tubulin (T9026) (MilliporeSigma); and anti-actin (MAB1501; EMD Millipore).

Histology and immunohistochemical staining. Paraffin-embedded mouse kidney sections (3-μm thickness) were prepared by a routine procedure (23). The sections were stained with PAS staining or MTS reagents by standard protocol. Immunohistochemical staining was performed according to the established protocol as described previously (16). Antibodies against Shh (sc-9024; Santa Cruz Biotechnology) and α-SMA (ab5694; Abcam) were used.

Immunofluorescence staining and confocal microscopy. Kidney cryosections were fixed with 3.7% paraformaldehyde for 15 minutes at room temperature. HKC-8 cells cultured on coverslips were fixed with cold methanol/acetone (1:1) for 10 minutes at –20°C. After blocking with 10% donkey serum for 1 hour, the slides were immunostained with primary antibodies against nephrin (20R-NP002; Fitzgerald Industries International), podocalyxin (MAB1556, R&D Systems), α-actinin-4 (ALX-210–356-c050; Enzo Life Sciences), CD31 (550274; BD Pharmingen), α-SMA (ab5694; Abcam), nestin (4760; Cell Signaling Technology), and PDGFR-β (3169, Cell Signaling Technology). These slides were then stained with Cy2- or Cy3-conjugated secondary antibody (Jackson ImmunoResearch Laboratories) and were mounted with Vectashield anti-fade mounting media (Vector Laboratories) using DAPI to visualize the nuclei. The stained slides were viewed under a Leica TCS-SL confocal microscope equipped with a digital camera.

Electron microscopy. Electron microscopy of kidney samples was carried out by routine procedures as described previously (22, 23). Briefly, mouse kidneys were perfusion fixed with 2.5% glutaraldehyde in phosphate-buffered saline by left cardiac ventricular injection and post-fixed in aqueous 1% OsO_4. Specimens were dehydrated through an ethanol series, infiltrated in a 1:1 mixture of propylene oxide/polybed 812 epoxy resin (Polysciences), and then embedded. Ultrathin sections were stained with 2% uranyl acetate, followed by 1% lead citrate. Sections were observed and photographed using a JEOL JEM 1210 transmission electron microscope (Peabody) at the Center for Biologic Imaging at the University of Pittsburgh.

X-Gal staining. For detecting functional β-Gal activity, OCT-embedded kidneys from the Gli1-LacZ–knockin reporter mice were cryosectioned into 7-μm sections and fixed with paraformaldehyde solution and then stained with standard 5-bromo-4-chloro-3-indolyl-β-D-galactopyranoside (X-Gal) for 2 days at 37°C. To quantify $LacZ^+$ cell number, 100× images were taken of the entire kidney from at least 3 different mice. The X-Gal staining protocol was provided by Ben Humphreys at the Washington University (St. Louis, Missouri, USA) and reported previously (43).

Statistics. All data are expressed as mean ± SEM. Statistical analysis of the data was performed using SigmaStat software (Jandel Scientific Software). Comparisons between groups were made using 1-way

ANOVA, followed by the Student-Newman-Keuls test. Comparisons between 2 groups were made using nonpaired 2-tailed Student's *t* test. Pearson's correlation was applied for analyzing the associations between serum Shh level and urinary protein, albumin/creatinine ratio, or glomerulosclerotic lesions. $P < 0.05$ was considered significant.

Study approval. All animal studies were performed according to the NIH *Guide for the Care and Use of Laboratory Animals* (National Academies Press, 2011) and using procedures approved by the Institutional Animal Care and Use Committee at the University of Pittsburgh. Studies involving human serum and kidney sections were approved by the Institutional Ethics Committee at the Affiliated Hospital of the Nanjing University of Chinese Medicine and the Nanfang Hospital at Southern Medical University as well as the Institutional Review Board at the University of Pittsburgh.

Author contributions

DZ and YL conceived and designed the study. DZ, HF, YH, SL, LZ, and LL carried out experiments. DZ, DBS, HF, and YL analyzed the data. DZ made the figures. DZ and YL drafted and revised the paper. All authors approved the final version of the manuscript.

Acknowledgments

This work was supported by the NIH grants DK064005 and DK106049 and NSFC grant 81521003. DZ is supported by NIH grant 1K01DK116816.

Address correspondence to: Youhua Liu, Department of Pathology, University of Pittsburgh, S-405 Biomedical Science Tower, 200 Lothrop Street, Pittsburgh, Pennsylvania, 15261, USA. Phone: 412.648.8253; Email: yhliu@pitt.edu.

1. Turin TC, et al. Proteinuria and rate of change in kidney function in a community-based population. *J Am Soc Nephrol*. 2013;24(10):1661–1667.
2. Webster AC, Nagler EV, Morton RL, Masson P. Chronic Kidney Disease. *Lancet*. 2017;389(10075):1238–1252.
3. Wetmore JB, Guo H, Liu J, Collins AJ, Gilbertson DT. The incidence, prevalence, and outcomes of glomerulonephritis derived from a large retrospective analysis. *Kidney Int*. 2016;90(4):853–860.
4. Fogo AB. Causes and pathogenesis of focal segmental glomerulosclerosis. *Nat Rev Nephrol*. 2015;11(2):76–87.
5. Brinkkoetter PT, Ising C, Benzing T. The role of the podocyte in albumin filtration. *Nat Rev Nephrol*. 2013;9(6):328–336.
6. Nagata M. Podocyte injury and its consequences. *Kidney Int*. 2016;89(6):1221–1230.
7. Warren AM, Knudsen ST, Cooper ME. Diabetic nephropathy: an insight into molecular mechanisms and emerging therapies. *Expert Opin Ther Targets*. 2019;23(7):579–591.
8. Ruggenenti P, Cravedi P, Remuzzi G. Mechanisms and treatment of CKD. *J Am Soc Nephrol*. 2012;23(12):1917–1928.
9. Levey AS, et al. Proteinuria as a surrogate outcome in CKD: report of a scientific workshop sponsored by the National Kidney Foundation and the US Food and Drug Administration. *Am J Kidney Dis*. 2009;54(2):205–226.
10. Reich HN, Troyanov S, Scholey JW, Cattran DC, Toronto Glomerulonephritis Registry. Remission of proteinuria improves prognosis in IgA nephropathy. *J Am Soc Nephrol*. 2007;18(12):3177–3183.
11. van den Belt SM, et al. Early Proteinuria Lowering by Angiotensin-Converting Enzyme Inhibition Predicts Renal Survival in Children with CKD. *J Am Soc Nephrol*. 2018;29(8):2225–2233.
12. Cravedi P, Ruggenenti P, Remuzzi G. Proteinuria should be used as a surrogate in CKD. *Nat Rev Nephrol*. 2012;8(5):301–306.
13. de Zeeuw D, Parekh R, Soman S. CKD treatment: time to alter the focus to albuminuria? *Adv Chronic Kidney Dis*. 2011;18(4):222–223.
14. Zhou D, Tan RJ, Liu Y. Sonic hedgehog signaling in kidney fibrosis: a master communicator. *Sci China Life Sci*. 2016;59(9):920–929.
15. Echelard Y, et al. Sonic hedgehog, a member of a family of putative signaling molecules, is implicated in the regulation of CNS polarity. *Cell*. 1993;75(7):1417–1430.
16. Zhou D, et al. Sonic hedgehog is a novel tubule-derived growth factor for interstitial fibroblasts after kidney injury. *J Am Soc Nephrol*. 2014;25(10):2187–2200.
17. Ding H, et al. Sonic hedgehog signaling mediates epithelial-mesenchymal communication and promotes renal fibrosis. *J Am Soc Nephrol*. 2012;23(5):801–813.
18. Bai Y, et al. Sonic hedgehog-mediated epithelial-mesenchymal transition in renal tubulointerstitial fibrosis. *Int J Mol Med*. 2016;37(5):1317–1327.
19. Yu J, Carroll TJ, McMahon AP. Sonic hedgehog regulates proliferation and differentiation of mesenchymal cells in the mouse metanephric kidney. *Development*. 2002;129(22):5301–5312.
20. Fabian SL, et al. Hedgehog-Gli pathway activation during kidney fibrosis. *Am J Pathol*. 2012;180(4):1441–1453.
21. Zou J, et al. Upregulation of nestin, vimentin, and desmin in rat podocytes in response to injury. *Virchows Arch*. 2006;448(4):485–492.
22. Zhou L, et al. Wnt/β-catenin links oxidative stress to podocyte injury and proteinuria. *Kidney Int*. 2019;95(4):830–845.
23. Dai C, Stolz DB, Kiss LP, Monga SP, Holzman LB, Liu Y. Wnt/beta-catenin signaling promotes podocyte dysfunction and

albuminuria. *J Am Soc Nephrol*. 2009;20(9):1997–2008.
24. Zhuo H, Zhou D, Wang Y, Mo H, Yu Y, Liu Y. Sonic hedgehog selectively promotes lymphangiogenesis after kidney injury through noncanonical pathway. *Am J Physiol Renal Physiol*. 2019;317(4):F1022–F1033.
25. He W, Kang YS, Dai C, Liu Y. Blockade of Wnt/β-catenin signaling by paricalcitol ameliorates proteinuria and kidney injury. *J Am Soc Nephrol*. 2011;22(1):90–103.
26. Reidy K, Kang HM, Hostetter T, Susztak K. Molecular mechanisms of diabetic kidney disease. *J Clin Invest*. 2014;124(6):2333–2340.
27. Alicic RZ, Johnson EJ, Tuttle KR. SGLT2 Inhibition for the Prevention and Treatment of Diabetic Kidney Disease: A Review. *Am J Kidney Dis*. 2018;72(2):267–277.
28. Kobayashi K, Forte TM, Taniguchi S, Ishida BY, Oka K, Chan L. The db/db mouse, a model for diabetic dyslipidemia: molecular characterization and effects of Western diet feeding. *Metab Clin Exp*. 2000;49(1):22–31.
29. Wiggins RC, et al. Glomerular disease: looking beyond pathology. *Clin J Am Soc Nephrol*. 2014;9(6):1138–1140.
30. Grahammer F, Schell C, Huber TB. The podocyte slit diaphragm--from a thin grey line to a complex signalling hub. *Nat Rev Nephrol*. 2013;9(10):587–598.
31. Torban E, et al. From podocyte biology to novel cures for glomerular disease. *Kidney Int*. 2019;96(4):850–861.
32. Zhou L, Liu Y. Wnt/β-catenin signalling and podocyte dysfunction in proteinuric kidney disease. *Nat Rev Nephrol*. 2015;11(9):535–545.
33. Wang D, Dai C, Li Y, Liu Y. Canonical Wnt/β-catenin signaling mediates transforming growth factor-β1-driven podocyte injury and proteinuria. *Kidney Int*. 2011;80(11):1159–1169.
34. Harris R. EGFR signaling in podocytes at the root of glomerular disease. *Nat Med*. 2011;17(10):1188–1189.
35. Ghayur A, Margetts PJ. Transforming growth factor-beta and the glomerular filtration barrier. *Kidney Res Clin Pract*. 2013;32(1):3–10.
36. Hsu HH, et al. Mechanisms of angiotensin II signaling on cytoskeleton of podocytes. *J Mol Med*. 2008;86(12):1379–1394.
37. Zhou L, et al. Multiple genes of the renin-angiotensin system are novel targets of Wnt/β-catenin signaling. *J Am Soc Nephrol*. 2015;26(1):107–120.
38. Kramann R, et al. Pharmacological GLI2 inhibition prevents myofibroblast cell-cycle progression and reduces kidney fibrosis. *J Clin Invest*. 2015;125(8):2935–2951.
39. Delgado I, Torres M. Coordination of limb development by crosstalk among axial patterning pathways. *Dev Biol*. 2017;429(2):382–386.
40. Pavenstädt H, Kriz W, Kretzler M. Cell biology of the glomerular podocyte. *Physiol Rev*. 2003;83(1):253–307.
41. Lu CC, et al. Role of podocyte injury in glomerulosclerosis. *Adv Exp Med Biol*. 2019;1165:195–232.
42. Xiao L, et al. Sustained Activation of Wnt/β-Catenin Signaling Drives AKI to CKD Progression. *J Am Soc Nephrol*. 2016;27(6):1727–1740.
43. Zhou D, et al. Fibroblast-Specific *β*-Catenin Signaling Dictates the Outcome of AKI. *J Am Soc Nephrol*. 2018;29(4):1257–1271.